Photoexcitation of nuclear isomers by (γ,γ') reactions

J. J. Carroll, M. J. Byrd, D. G. Richmond, T. W. Sinor, K. N. Taylor, W. L. Hodge,*
Y. Paiss,† C. D. Eberhard, J. A. Anderson,‡ and C. B. Collins
Center for Quantum Electronics, University of Texas at Dallas, Richardson, Texas 75083

E. C. Scarbrough and P. P. Antich
The University of Texas Southwestern Medical Center at Dallas, Dallas, Texas 75235

F. J. Agee, D. Davis, G. A. Huttlin, K. G. Kerris, M. S. Litz, and D. A. Whittaker
Aurora Simulator Facility, Harry Diamond Laboratories, Adelphi, Maryland 20783
(Received 21 April 1989)

Photoexcitation of the isomers of 19 nuclides was examined in this work. Four accelerators were used as sources of bremsstrahlung to expose the samples and end-point energies covered the range from 0.5 to 11 MeV. No evidence was found for nonresonant processes of excitation. However, more than half the cases showed enhanced channels for the resonant photoexcitation of isomers with integrated cross sections approaching 10^{-21} cm^2 keV. These results are three to four orders of magnitude larger than values usually characterizing (γ,γ') reactions.

INTRODUCTION

Because the photon carries relatively little momentum, (γ,γ') reactions must proceed through resonant channels for excitation with rather narrow widths. This aspect distinguishes photoexcitation from related processes such as (γ,n). The generation of an additional particle with which to conserve momentum provides a threshold of energy above which all incident photons can mediate the reaction. This facilitates the study of processes such as (γ,n) by increasing product yields and richly detailed results have been reported in the literature.[1] In contrast, the difficulties in exciting the narrow resonances for (γ,γ') reactions have inhibited investigations and relatively few results have been published in the past 50 years over which such processes have been known.[2,3]

In the region of energies from 0.1 to 10.0 MeV photon sources emit continuous spectra and the opportunity to probe (γ,γ') reactions with a tunable source of narrow width does not exist at practical levels of intensity. Even experiments designed to use γ sources are actually done with continua because of the degradation of the line spectra by Compton scattering in the real geometries employed.

The most tractable (γ,γ') reactions for study are those for the photoexcitation of isomeric states. The product lives long enough to be readily examined after termination of the input irradiation. The archetypical case has been the reaction ^{111}Cd$(\gamma,\gamma')^{111}$Cd^m exciting the 48.6 min isomer. Three of the most recent measurements of the integrated cross section $\sigma\Gamma$ were conducted in 1979, 1982, and 1987 with results of 35, 5.8, and 14 as reported in Refs. 4–6, respectively, in the usual units of 10^{-29} cm^2 keV. Probable errors were quoted as varying only from 7% to 14% and yet, no two of the measurements were even within a factor of 2 of each other. This discrepancy led to the curious suggestion[5] that some unknown mechanism for *nonresonant* nuclear absorption generally dominates the excitation step. Although fundamental considerations insist that for energies below the thresholds of neutron evaporation all (γ,γ') reactions must first excite bound nuclear states, the belief continued to spread that nonresonant processes were involved. The (γ,γ') reactions of ^{113}In, ^{87}Sr, and ^{180}Ta^m were all subsequently attributed to the unidentified nonresonant process.[7,8]

Recently, the technology has become available[9,10] to measure the spectrum of a source of pulsed bremsstrahlung, together with greatly improved computer codes[11,12] with which to calculate spectra for realistic geometries. These advances made it possible to resolve[13] the persisting controversies in the reaction ^{111}Cd$(\gamma,\gamma')^{111}$Cd^m, as well as those[14] in ^{115}In$(\gamma,\gamma')^{115}$In^m. As expected, it was found[13,14] that both ^{115}In^m and ^{111}Cd^m were excited by resonant absorption through intermediate gateway states near 1 MeV that were broadened by their short lifetimes. The sharp onset of the (γ,γ') reactions with increasing energy relegated to less than 3% any contributions from nonresonant processes and indicated that the gateway states were reasonably well connected by radiative transitions to both the ground states and the isomers. It appears that the principal cause for the large discrepancy between previous measurements was the difficulty in adequately characterizing the spectra of the irradiation. This was particularly true for radioactive sources since all spectral contributions away from the source lines were necessarily due to Compton continua generated by scattering in the irradiation environment.

The model for the photoexcitation of isomeric nuclei confirmed in recent work[13,14] is shown in Fig. 1. Only two gateway levels are drawn as examples and the number actually participating depends upon the sequence of energy levels and transition probabilities for the particu-

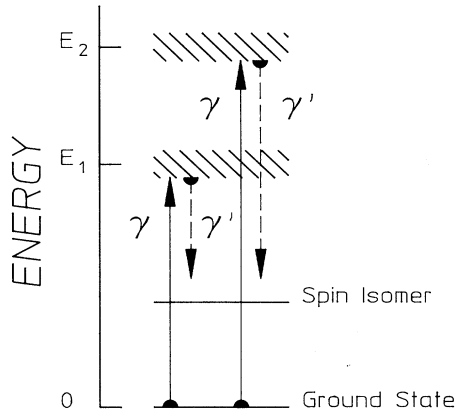

FIG. 1. Schematic representation of the (γ,γ') reactions used to populate isomeric states in these experiments. The resonant absorption of bremsstrahlung x rays, denoted as γ, excite populations of gateway states. Two are shown at excitation energies of E_1 and E_2 but the actual number will vary for each nuclide. Parts of the populations of the gateway states make transitions to the final state either directly or as part of a cascade of radiative transitions ending on the final state as indicated by the dashed arrows.

lar nucleus being considered. In the resolution of previous conflicts in ^{111}Cd and ^{115}In the values finally confirmed lay within the scatter of earlier measurements and generally agreed with nuclear parameters measured by other means.[15] However, when studies were extended to the deexcitation of an isomeric sample through the reverse of the sequence shown in Fig. 1, unexpectedly large results were obtained.[16] In contrast to values of a few 10's$\times 10^{-29}$ cm^2 keV measured for the excitation of isomers, a value of $40\,000\times 10^{-29}$ cm^2 keV was reported[16] for the deexcitation of ^{180}Ta^m with a 6 MeV linac. The reaction ^{176}Lu$(\gamma,\gamma')^{176}$Lu^m was reported to proceed with an integrated cross section of comparable magnitude.[17] The strength of the dumping reaction ^{180}Ta$^m(\gamma,\gamma')^{180}$Ta was confirmed[18] with bremsstrahlung from the injector to the Darmstadt superconducting electron accelerator operated at 12 different end-point energies. Two gateway levels for ^{180}Ta$^m(\gamma,\gamma')^{180}$Ta were reported with integrated cross sections that totaled to $47\,000\times 10^{-29}$ cm^2 keV.

It was the purpose of the work reported here to examine the systematics of these giant resonances for the photoexcitation of isomeric states to determine whether such results were curiosities associated only with ^{176}Lu and ^{180}Ta^m or whether they were part of more generally prevalent phenomena. A secondary objective was to learn whether the large integrated cross sections were the results of a large number of reaction channels of more conventional size or rather, a few of unprecedented magnitude.

Unfortunately, the type of electron accelerators that provided bremsstrahlung spectra with end-point energies that were chosen at will in classical investigations[19] of (γ,γ') reactions is no longer available in North America. For the experiments reported here we could arrange access only to a combination of accelerators, some with limited variability of end-point energies such as DNA/PITHON at Physics International and DNA/Aurora at Harry Diamond Laboratories. Between the ranges of energies available from those machines we used two medical linacs having fixed end points of 4 and 6 MeV. This enabled us to examine the photoexcitation of 19 isomeric nuclei, most of them over the range from 0.5 to 11 MeV. The variety of accelerators and locations minimized the possibility of introducing any systematic bias which might have been associated with any particular machine or its environment.

METHODOLOGY

Analytic approach

The normalized activation $A_f(E_0)$ of a sample per unit photon flux Φ_0 produced with a bremsstrahlung source having an endpoint E_0 can be written as

$$A_f(E_0)\equiv\frac{N_f}{N_i\Phi_0}=\sum_j(\sigma\Gamma)_{fj}F(E_j,E_0)\ , \tag{1}$$

where N_i and N_f are the populations of initial and final nuclear states, respectively. In Eq. (1), $(\sigma\Gamma)_{fj}$ is the integrated cross section for the excitation of N_f through the jth gateway state as shown in Fig. 1. The function $F(E_j,E_0)$ is the spectral function describing the relative intensity at the photon energy, E_j, normalized so that

$$\int_0^{E_0}F(E,E_0)dE=1\ . \tag{2}$$

The normalized activation can be useful as a sensitive indication of the opening of (γ,γ') channels whenever photons of the requisite energies E_j become available. A change of the end-point energy E_0 of the bremsstrahlung spectrum modulates the spectral intensity function $F(E_j,E_0)$ in Eq. (1) at all of the important gateway energies, E_j. The largest effect in the excitation function occurs when E_0 is increased from a value just below some gateway at $E_j=E_k$ to one exceeding it so that $F(E_j,E_0)$ varies from zero to some finite value. In earlier work[19] plots of quantities equivalent to Eq. (1) as functions of the end-point energies of the irradiating spectra showed very pronounced activation edges which appeared as sharp increases at the energies, E_j, corresponding to excitation of new gateways.

In the work reported here the ratios of activation N_f/N_i to the irradiation dose were examined as functions of E_0. The relationships between dose, which was measured directly, and Φ_0, which had to be derived from it, depended upon $F(E,E_0)$. The normalization to dose rather than Φ_0 was chosen to avoid any dependence of the features of the excitation function upon simulation models.

Experimental details

Sample materials were exposed to photons having energies up to 1.5 MeV with the DNA/PITHON nuclear simulator at Physics International. This device was a flash x-ray source using a single transmission line pulsed by a Marx generator. Since the end-point energy could be varied to some degree by changing the charging voltage of the Marx, photoexcitation from 0.5 to 1.5 MeV could be investigated with a resolution limited by the available end-point energies. The samples were placed in front of a converter foil which terminated the transmission line, and were aligned to face the photon flash. These were exposed in complex packages to activate several materials in each shot from DNA/PITHON, an important detail since the pulse repetition frequency was less than 1 h^{-1}. All the sample packages were backed with thermoluminescent dosimeters (TLD's) to measure the dosage which each target received.

The 1.5 to 6 MeV range was studied with two fixed end-point medical linacs at the Department of Radiology of the University of Texas Southwestern Medical Center at Dallas. Irradiations with nominal 4 MeV bremsstrahlung were obtained with a Varian Clinac 4/100 linac which provided a dose rate of 200 rad(H_2O) min^{-1} at 101.2 cm from the converter target. Bremsstrahlung having a nominal end point of 6 MeV was obtained with a Varian Clinac 1800 linac operating in the 6 MeV mode. This device produced 400 rad(H_2O) min^{-1} at 101.5 cm from the converter target. For both machines, the dose rate was determined by in-line ion chambers whose calibrations were directly traceable to NIST. Samples were exposed in packages confined to the region of most uniform dose distribution.

Irradiations in the 6 to 11 MeV range were provided with the DNA/Aurora nuclear simulator,[20] located at the Harry Diamond Laboratories. Powered by a Marx bank, photons were generated by converter foils which terminated four separate transmission lines. These converged on a target volume of roughly 0.1 m^3 in which the photon field was most intense. Again, the Marx charging voltage was varied to provide irradiations with different end-point bremsstrahlung. Samples were positioned in the high intensity spot and were backed by TLD's. These packages were oriented to face the centerline of the machine rather than any particular transmission line.

The spectra of these four machines have been well characterized, particularly the linacs which are committed to patient treatment. Photon spectra of the DNA/PITHON and DNA/Aurora accelerators were obtained through use of the Integrated TIGER Series (ITS) computational program.[12] They were calibrated by matching the end-point energy and the total dosage to the shape of the calculated spectrum. The DNA-PITHON device could also be cross calibrated by the activation technique described in Refs. 9 and 10. Typical spectra are given in Fig. 2 which shows the relative intensity function $F(E,E_0)$, on the meshes of energies for which data were available. For the DNA/PITHON shot shown, $\Phi_0=4\times10^{14}$ photons cm^{-2} and for the DNA/Aurora shot, $\Phi_0=5\times10^{13}$ photons cm^{-2}.

The output spectra of the medical linacs employed in this work were calculated with the EGS4 code developed at SLAC.[11] Unfortunately, the relative spectral intensity functions of these devices that were found in the literature[21] contained a computational artifact. To minimize that feature the spectra had to be modeled as part of this work. Results are shown in Fig. 3, together with the

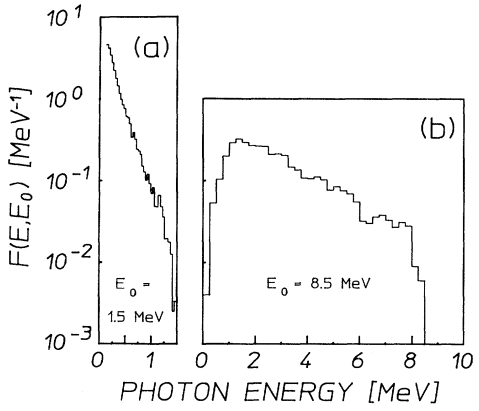

FIG. 2. Relative spectral intensities $F(E,E_0)$ of the bremsstrahlung typically produced by nuclear simulators used to irradiate samples in these experiments. The curves are normalized so that their areas are unity. The devices employed were (a) DNA/PITHON, with an end point of $E_0=1.5$ MeV; (b) DNA/Aurora, with an end point of $E_0=8.5$ MeV.

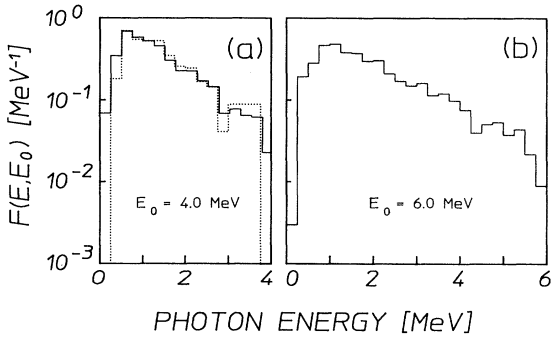

FIG. 3. Relative spectral intensities $F(E,E_0)$ of the bremsstrahlung produced by the medical linacs used to irradiate samples in these experiments. The curves are normalized so that their areas are unity. The solid lines indicate empirical fits to the calculated spectra as discussed in the text. The devices employed were as follows: (a) Varian Clinac 4/100, with a nominal end point of 4 MeV. The dotted curve shows the spectrum obtained from Ref. 21 that contains a computational artifact at about 3 MeV. (b) Varian Clinac 1800, operated in the nominal 6 MeV end-point mode.

literature values for a typical case.[21] The total fluxes at 100 cm were 3.23×10^{11} photons cm^{-2} min^{-1} for the nominally 4 MeV device, and 5.35×10^{11} photons cm^{-2} min^{-1} for the Clinac 1800 in the 6 MeV mode.

The isotopes studied in these experiments are listed in Table I along with the relevant physical parameters. The techniques employed to obtain measurements of activation depended upon the lifetimes of the isomeric states and whether or not these were long enough to transport the irradiated samples by simple means.

Isomers of the first nine nuclides listed in Table I have half-lives of less than 3 min and therefore required special treatment. These samples consisted of either powders or metallic foils enclosed in cylindrical polyethylene vials which were pneumatically transported to a well-type NaI(Tl) detector after exposure. The low energy resolution of this detector necessitated some care in the identification of the prominent features in the pulse height spectra. In all cases, confirmations that these were the fluorescence signatures of the isomers were made by determining the half-lives of the product populations. This was made possible by simultaneously acquiring data

TABLE I. Summary of isomeric nuclei studied. Nuclei marked * were present in isotopically enriched samples. In the sample column, *R* refers to samples contained in vials transferred pneumatically, *P* to flat planchettes, *F* to metallic foils, and *B* to scintillation bottles. The ^{180}Ta sample consisted of a dusting of oxide on a thin aluminum plate, referred to by *D*. In the case of the ^{176}Lu sample, β^- particles were observed instead of fluorescence photons; the NA in the transparency column indicates that this factor was not applicable for ^{176}Lu.

Nuclide	Abundance (%)	Sample form	$T_{1/2}$	Principal fluorescence (keV)	Transparency (%)
^{167}Er	91.54*	Er_2O_3 (*R*)	2.28 sec	207.79 (41.70%)	57.90
^{79}Br	50.69	LiBr (*R*)	4.86 sec	207.20 (75.80%)	84.90
^{191}Ir	37.30	Ir (*R*)	4.94 sec	129.43 (25.70%)	10.50
^{197}Au	100.00	Au (*R*)	7.80 sec	279.11 (73.00%)	92.70
^{89}Y	100.00	YF_3 (*R*)	16.06 sec	909.15 (99.14%)	94.70
^{77}Se	94.38	Se (*R*)	17.45 sec	161.92 (52.40%)	72.28
^{179}Hf	13.63	HfO_2 (*R*)	18.68 sec	214.31 (94.20%)	52.40
^{199}Hg	16.90	Hg_2Cl_2 (*R*)	43.20 sec	158.40 (53.00%)	43.96
^{137}Ba	11.74	BaF_2 (*R*)	153.12 sec	661.66 (90.10)	95.50
^{111}Cd	12.80	Cd (*F*)	48.6 min	245.49 (94.00%)	76.35
^{113}In	4.30	In (*F*)	1.66 h	391.69 (64.20%)	98.30
^{87}Sr	7.00	SrF_2 (*P*)	2.81 h	388.40 (82.30%)	95.78
^{176}Lu	2.59	$LuCl_3$ (*B*)	3.63 h	beta	NA
^{115}In	95.70	In (*F*)	4.49 h	336.26 (45.80%)	98.00
^{180}Ta	4.00*	TaO_2 (*D*)	8.15 h	55.79 (36.00%)	100.00
^{135}Ba	6.60	BaF_2 (*P*)	1.20 d	268.27 (15.60%)	94.33
^{195}Pt	33.80	Pt (coin)	4.02 d	98.88 (11.40%)	4.76
^{117}Sn	7.70	Sn (*F*)	13.6 d	158.56 (86.40%)	92.89
^{123}Te	0.908	Te (*P*)	119.7 d	158.99 (84.00%)	62.68

through two Ortec 918A ADCAM multichannel buffers controlled by a personal computer. While one ADCAM served to produce a pulse height spectrum, the other collected a record of the total counts received in the preset dwell interval as a function of time. A typical example of the data obtained in this way is given in Figs. 4(a) and 4(b), showing measurements for the isomer $^{167}Er^{m}$.

The remaining nuclides in Table I had half-lives longer than 48.6 min, and could be transported by hand to a nearby solid-type NaI(Tl) detector for counting. Samples containing particularly long-lived isomers like 119.7 d $^{123}Te^{m}$ and 13.61 d $^{117}Sn^{m}$ were transported to the Center for Quantum Electronics where they were counted using a high-purity, *n*-type germanium (HPGe) detector. The physical form of the materials in this slower class consisted either of thin metallic disks or flat polyethylene planchettes containing metallic chips or chemical compounds.

Since the HPGe detector provided greater resolution it was not necessary to monitor the time decay in detail. For some samples, however, energy spectra were acquired after several different elapsed times to provide additional confirmation of the product signature. For example, a pulse height spectrum of $^{123}Te^{m}$ after a 6 MeV exposure is shown in Fig. 5(a). The fluorescence line at 159 keV is well defined and gives 5% counting statistics. Since this was the longest-lived isomer ever reported to be excited by a (γ,γ') reaction, the time decay was experimentally determined from a sequence of energy spectra taken after a 6 MeV exposure. The decay of the count rate is shown in Fig. 5(b). A fit to these data gives a half-life which is in excellent agreement with the literature value.

The nuclide, ^{176}Lu, was examined with a different

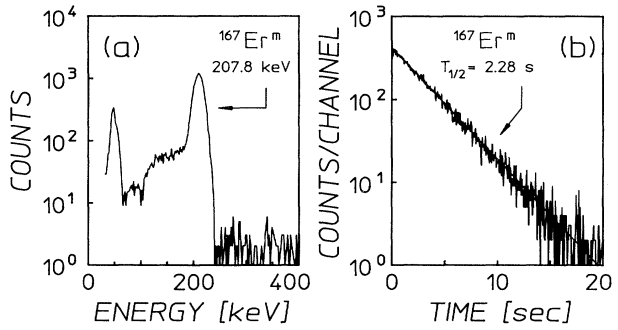

FIG. 4. Fluorescence data for the 207.8 keV line from the decay of $^{167}Er^{m}$ following a 6 MeV exposure. These were obtained with a 7.6 cm×7.6 cm diameter NaI(Tl) detector having a 5.1 cm×2.5 cm diameter well. The sample was irradiated for 25 sec. (a) Pulse height spectrum obtained with a counting period 5 sec in duration after a transport time of 2.06 sec from the end of irradiation to the start of counting. (b) Total counting rates observed in successive dwell intervals of 0.05 sec as a function of the time elapsed from the start of the counting interval following a 6 MeV exposure. The solid line indicates the literature value of the half-life, 2.28 sec.

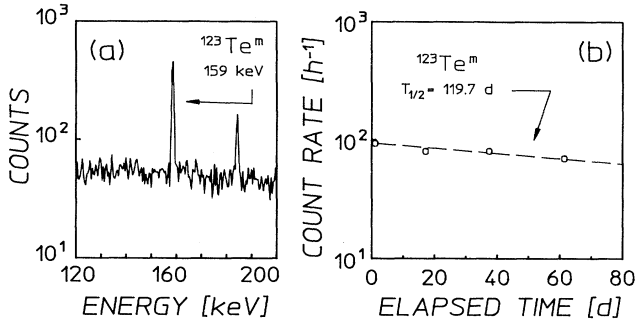

FIG. 5. Fluorescence data for the 159 keV line from the decay of $^{123}Te^{m}$ following a 6 MeV exposure. These were obtained with an *n*-type high-purity germanium detector. The sample was irradiated for 2 h. (a) Pulse height spectrum obtained with a counting period of 10 h duration after a delay from the finish of the irradiation of 22.98 h. (b) Points represent the counting rates in pulse height spectra at different elapsed times. The sizes of the symbols are comparable to one standard deviation and the counting periods were all 10 h. The dashed line shows the literature value for half-life of 119.7 d.

detection scheme. Since the isomer does not return to the ground state by a radiative transition, the number of excited nuclei must be measured by the detection of either β^- particles or the photons from the daughter nucleus. The ground state β^- decays with an end-point energy of 565 keV and the isomer β^- decays with end-point energies of 1313 keV (39.6%) and 1225 keV (60.4%). This difference allowed the use of a Cerenkov detector. Samples consisting of $LuCl_3$, dissolved in distilled water, were contained in polyethylene scintillation bottles. The Cerenkov threshold in water is about 250 keV and β^- particles emitted in the decay of the isomeric states were nearly 10 times more efficient in producing Cerenkov events than those emitted from ground state nuclei. Photons from these events were measured in coincidence, thereby recognizing only signals from the Cerenkov photons produced by single β^- particles. The detector was calibrated with ^{40}K decays from a KCl solution of known activity, since the resulting β^- particles had roughly the same end-point energy as those from $^{176}Lu^{m}$. In these measurements, the individual count rates were monitored to avoid contributions from accidental coincidences triggered by separate β^- events or by thermoluminescence from the material of the bottle. A fit to the experimental data shown in the typical spectrum of Fig. 6 produced a value for the half-life for $^{176}Lu^{m}$ of 3.58±0.05 h, which is in good agreement with the literature value of 3.63 h.

The yields of each of the final state populations were determined from the numbers of counts collected in the corresponding peaks in pulse height spectra. These raw data were then corrected in a standard manner for the photopeak detector efficiency, the fraction of fluorescence photons per decay, and the finite times of sample transport and counting. The latter factor used literature values of the half-lives.[15] It was also necessary to account

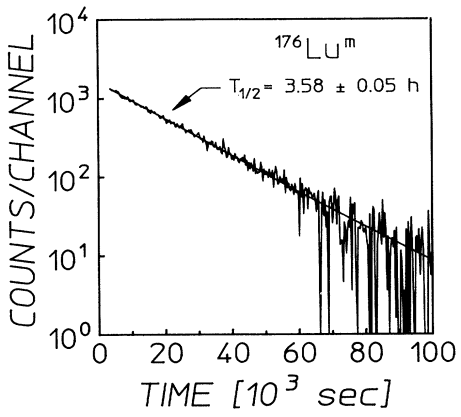

FIG. 6. Data typical of the counting rates observed in successive dwell time intervals of 320 sec for $^{176}Lu^m$ as a function of the time following a 6 MeV exposure. The sample was irradiated for 40 min and the delay time to the beginning of the counting was 53 min. A fit to the data is shown by the solid line for a half-life of 3.58±0.05 h, in good agreement with the literature value of 3.63 h.

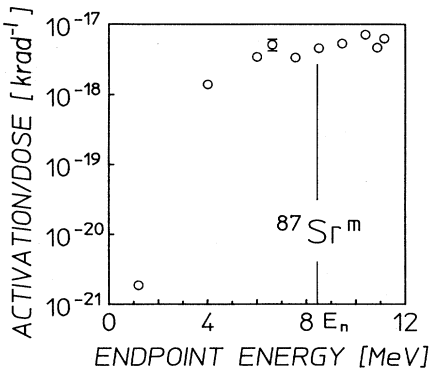

FIG. 7. Normalized activation obtained from irradiations with all four accelerators for $^{87}Sr^m$. The size of the symbols is comparable to one standard deviation except where error bars are explicitly shown. The point at 1.2 MeV determined from a DNA/PITHON exposure is an upper bound on the excitation since no fluorescence photons were observed above the level of background. The vertical line indicates the neutron evaporation threshold at $E_n = 8.4$ MeV.

for some attenuation of the fluorescence photons within the samples themselves because of absorption and scattering events. This effect was accommodated by Monte Carlo calculations of a transparency factor for each sample. These corrections were confirmed by comparing the activations obtained from targets containing identical materials, but in different geometries.

RESULTS

Strontium as a benchmark

Normalized activation measurements obtained from all four accelerators for $^{87}Sr^m$ are shown in Fig. 7, which also indicates the threshold energy for (γ,n) reactions, E_n at 8.428 MeV. The datum at 1.2 MeV represents an upper limit since no fluorescence photons were observed above the background level. Although lacking in resolution in the critical range from 1.2 to 6 MeV, the data allow several conclusions to be drawn about the photoexcitation process. First is that there is no evidence to support the participation of any nonresonant processes. This type of mechanism, if present, would be heavily dependent upon the density of nuclear states, which rises sharply at energies approaching E_n. The slow increase in the excitation function above 6 MeV relative to the change seen below 4 MeV precludes this as the dominant means of photoexcitation.

The large increase in normalized activation from 1.2 to 4 MeV indicates that at least one resonant gateway of significant magnitude lies in that range. The experimental resolution, however, does not allow a clear observation of the activation edges so the details of these states cannot be directly determined.

Fortunately, the isomer $^{87}Sr^m$ is distinguished by the degree to which its photoexcitation has been characterized in the literature. An early work[19] examined the production of this isomer by bremsstrahlung with end points which could be varied up to 3 MeV. The tunability of that device allowed three distinct gateways to be identified at 1.22, 1.88, and 2.66 MeV, and their integrated cross sections to be measured. In the usual units of 10^{-29} cm^2 keV, these were found to be 8.5^{+4}_{-3}, 16^{+8}_{-5}, and 380^{+200}_{-100}, respectively.

Figure 8(a) shows the ^{87}Sr data together with the nor-

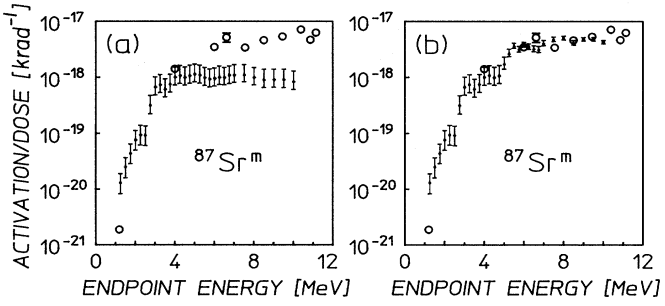

FIG. 8. Open circles plot normalized activations obtained from irradiations with all four accelerators for $^{87}Sr^m$ as previously shown in Fig. 7. Also displayed as solid bars are excitation functions calculated from Eq. (1) for the following: (a) Expected photoexcitation through the three known gateways of Ref. 19. The error bars indicate the uncertainties in the measurements of $(\sigma\Gamma)$ in that work. (b) Expected photoexcitation through the three known gateways plus that of a hypothetical state near 5 MeV with an integrated cross section on the order of 4000×10^{-29} cm^2 keV. The error bars indicate only the uncertainties in the measured $(\sigma\Gamma)$ of Ref. 19.

malized activations that should have been excited through the known gateways by photons with energies below 4 MeV. These values were calculated from Eq. (1) for different end-point energies by using typical bremsstrahlung spectra scaled from those shown in Fig. 3. The composite graph produced in this way exhibits the required activation edges at 1.22 and 2.66 MeV in agreement with the actual measurements. No edge is apparent at 1.88 MeV, but this is due to the comparable magnitude and proximity of this level to the one at 1.22 MeV. The correlation of the expected values near 4 MeV with the datum there indicates that no new states are required to explain all of the normalized activation obtained with the 4 MeV linac.

The data above 6 MeV in Fig. 8(a) significantly exceed the photoexcitation which could have been produced through the three known gateways. This extra activation must have therefore represented (γ,γ') reactions which proceeded through one or more unidentified levels. The simplest picture which matches the data is that of a single gateway near 5 MeV with an integrated cross section of the order of 4000×10^{-29} cm^2 keV. The normalized activation expected from this state, as well as those previously identified, is shown in relation to the experimental data in Fig. 8(b).

The nuclide ^{87}Sr provides a benchmark for other (γ,γ') studies since this is the only instance in which the current work can be compared with earlier experiments over a significant range of energies. It is apparent that the present measurements of the photoexcitation of ^{87}Sr^m below 4 MeV are completely explained by resonant absorption of photons through gateways already reported in the literature.[19]

Nuclide survey

All of the nuclei of Table I were irradiated with at least three of the four accelerators available. In all cases the general phenomenology seen in Fig. 7 was reproduced, but with considerable variance in the heights of the plateaus of activation reached at the higher energies. A typical example is shown in Fig. 9, which displays data obtained for the isomer ^{167}Er^m along with those for ^{87}Sr^m. Several interesting aspects are apparent. Although the normalized activations achieved with ^{167}Er nuclei are nearly two orders of magnitude larger than those of the ^{87}Sr benchmark, both isomers display similarly slow increases in activation above 6 MeV. This is surprising since nonresonant processes might be expected to be more significant for the photoexcitation of a nucleus as massive as ^{167}Er. Nevertheless, resonant absorption appears to be the dominant means of isomeric production for this nucleus as it was for the benchmark nuclide. The increase in normalized activation between the 4 and 6 MeV data strongly implies that a large gateway lies in this range. The magnitude of the data near 1.2 MeV suggests that a smaller activation edge lies at lower energy.

The measurements obtained from several nuclides, ^{77}Sr, ^{79}Br, ^{111}Cd, and ^{115}In allowed the identification of resonances below 1.5 MeV. The integrated cross sections of those were found to be on the order of 1 to 10×10^{-29} cm^2 keV, and results were reported previously.[9,10,13,14] The isotope, ^{179}Hf, while not providing such detailed information, did indicate an activation edge at about 1.1 MeV for its 18.7 sec isomer ^{179}Hf^m. Its excitation function is displayed in Fig. 10 and again the relatively slow

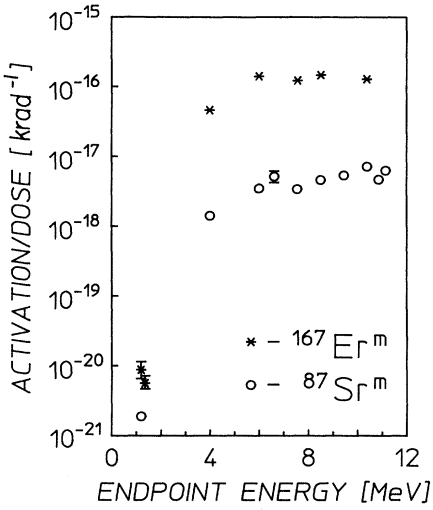

FIG. 9. Normalized activation obtained from irradiations with all four accelerators for ^{167}Er^m. Also included for the purpose of comparison are those values for ^{87}Sr^m. The size of the symbols is comparable to one standard deviation except where error bars are explicitly shown. The point at 1.2 MeV for ^{87}Sr^m determined from a DNA/PITHON exposure is an upper bound on the excitation since no fluorescence photons were observed above the level of background. The neutron evaporation thresholds for ^{167}Er and ^{87}Sr are 6.4 and 8.4 MeV, respectively.

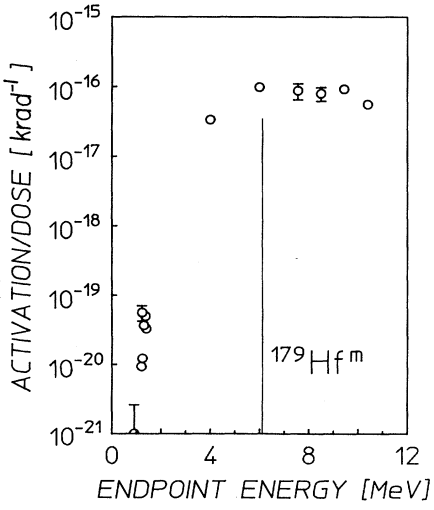

FIG. 10. Normalized activation obtained from irradiations with all four accelerators for 18.7 sec ^{179}Hf^m. The size of the symbols is comparable to one standard deviation except where error bars are explicitly shown. The vertical line indicates the neutron evaporation threshold at $E_n = 6.1$ MeV.

rise at high energies suggests resonant photoexcitation even for this large nucleus.

The absence of any evidence for nonresonant excitation made it useful to tabulate the results of this work in terms of an effective integrated cross section $(\sigma\Gamma)$, which was a weighted average of the actual values appearing in Eq. (1),

$$(\sigma\Gamma)\equiv\sum_j(\sigma\Gamma)_{fj}\frac{F(E_j,E_0)}{F(2.125,E_0)}\ . \tag{3}$$

The choice of normalizing the relative intensities to 2.125 MeV was arbitrary. However, since the excitation enegies of all of the dominant gateways exceeded 2.125 MeV and since $F(2.125,E_0)>F(E_j,E_0)$ for those gateways, the ratio used to weight individual $(\sigma\Gamma)_{fj}$ in Eq. (3) was always less than unity. This insured that the effective $(\sigma\Gamma)$ was not greater than the sum of all integrated cross sections for a particular nuclide. Substitution of Eq. (3) into Eq. (1) gives

$$(\sigma\Gamma)=\frac{N_f}{N_i\Phi_0F(2.125,E_0)}\ , \tag{4}$$

which in turn shows the effective $(\sigma\Gamma)$ to be the value that would have been necessary for a gateway at 2.125 MeV to produce the observed activation. The results are shown in Table II for the two different values of E_0 of the bremsstrahlung from the two linacs.

Neutron excitations

All of the accelerators used, other than DNA/PITHON, were capable of evaporating neutrons from their environments. Since neutrons can also excite nuclei into their isomeric states it was important to determine the amount of normalized activation which was attributable to these particles. In principle, two types of neutron reactions could have occurred: inelastic (n,n') reactions which would have required hot neutrons and neutron capture (n,γ) processes driven by fluxes of thermal or epithermal neutrons.

Contributions to the observed activations from (n,γ) reactions could be directly determined. The thermal neutron fluxes were measured by irradiating two thin indium foils, one of which was shielded from thermal neutrons by a cadmium cover. In accordance with standard techniques,[22] energy spectra obtained from these foils were examined after exposure for photons from the isomer $^{116}In^m$, which is produced by a branch of the reaction $^{115}In(n,\gamma)^{116}In^{m,g}$. In all cases such activations were negligible. For example, the magnitudes of the fluorescence lines observed in both the bare and the shielded

TABLE II. Summary of experimental results. The quantity ΔJ is the change in spin between ground state and isomer. For both 4 and 6 MeV irradiations, the integrated cross sections of a single gateway state at the reference energy of 2.125 MeV are given as $(\sigma\Gamma)$ and have been corrected for thermal and epithermal neutron contaminations. The ratio of 6 MeV values to those at 4 MeV are given as κ_1. The ratio of integrated cross sections obtained from 10.4 MeV to 6 MeV measurements is κ_2. Also given is the fraction of thermal and epithermal neutron contamination in the total activation, $A_n/A_{\rm tot}$. The comment NA is used in the column for $A_n/A_{\rm tot}$ when no naturally abundant parent is available for (n,γ) reactions. An entry NA in the κ_2 column indicates that this information is not currently available.

		4 MeV		6 MeV			
Nuclide	ΔJ	$(\sigma\Gamma)$ (10^{-29} cm^2 keV)	$A_n/A_{\rm tot}$ (%)	$(\sigma\Gamma)$ (10^{-29} cm^2 keV)	$A_n/A_{\rm tot}$ (%)	κ_1	κ_2
^{167}Er	3	4 600±110	0.01	34 000±360	0.32	7.4	1.0
^{79}Br	3	660±17	NA	1 900±23	NA	2.9	1.5
^{191}Ir	4	7 600±610	NA	36 000±960	NA	4.7	NA
^{197}Au	4	2 600±40	NA	13 000±64	NA	5.0	NA
^{89}Y	4	9±5	NA	260±8	NA	29	2.9
^{77}Se	3	330±4	0.03	6 500±32	0.76	20	NA
^{179}Hf	4	9 400±120	0.04	25 000±110	6.41	2.7	1.1
^{137}Ba	4	330±23	<0.01	1 900±23	0.07	5.8	1.4
^{199}Hg	6	260±10	0.05	1 400±42	5.40	5.4	NA
^{111}Cd	5	920±12	<0.01	2 500±44	0.07	2.7	NA
^{113}In	4	1 300±59	NA	4 700±180	NA	3.6	0.71
^{87}Sr	4	390±13	<0.01	870±18	0.89	2.2	2.3
^{176}Lu	6	14 000±95	0.01	35 000±2 300	1.51	2.5	NA
^{115}In	4	1 800±16	NA	6 700±14	NA	3.7	1.5
^{180}Ta	8	18 000±6 600	NA	35 000±650	NA	1.9	NA
^{135}Ba	4	1 300±62	<0.01	6 000±110	0.39	4.6	4.0
^{195}Pt	4	3 000±160	<0.01	14 000±220	0.03	4.7	NA
^{117}Sn	5	320±47	<0.01	880±26	0.07	2.8	0.84
^{123}Te	5	4 200±730	<0.01	6 800±320	1.45	1.6	NA

samples allowed the determination of the thermal neutron flux of 12 neutrons cm^{-2} sec^{-1} in the 6 MeV linac environment. The contributions to the activations from thermal neutrons are summarized in Table II for each of the 19 nuclides studied.

Because of a beryllium window used in the construction of the 6 MeV linac, that environment had the largest neutron flux. Nevertheless, the results of Table II show that under no conditions did the thermal neutrons contribute more than a few percent of the activation. In most cases neutron contamination represented a few $\times 10^{-4}$ fraction of the observed activations from the 6 MeV linac. The fast neutron flux was expected to be even less important and attempts to record any flux with the (n,p) reactions of ^{46}Ti, ^{47}Ti, and ^{58}Ni were completely negative. Calculations indicated a flux of fast neutrons from the photodisintegration of environmental sources consistent with this negative and limited contamination from (n,n') reactions to tenths of a percent.

CONCLUSIONS

The principal conclusion of this work is that some of the integrated cross sections for exciting isomers can be extraordinarily large, approaching 10^{-21} cm^2 eV. This is about three to four orders of magnitude larger than what has been usually reported in the past.

Typified by the reaction $^{167}\mathrm{Er}(\gamma,\gamma')^{167}\mathrm{Er}^m$, these enhanced processes seem to occur through discrete gateways or through narrow bands of gateway states. The data of Fig. 9 for ^{167}Er have a compelling resemblance to those for the excitation of ^{87}Sr which is known to occur through a few discrete levels. The same sharp jump in activation with increasing x-ray end point is followed by relatively level yield up to 11 MeV. It is possible to fit the data for ^{167}Er with a single gateway near 4 MeV but this is not a unique choice. The excitation function for the reaction $^{179}\mathrm{Hf}(\gamma,\gamma')^{179}\mathrm{Hf}^m$ shown in Fig. 10 also seems compelling in suggesting a single jump in activation at energies below 4 MeV. Table II shows that more than half of the 19 reactions studied had (γ,γ') reaction channels producing isomers with integrated cross sections greater than 1000×10^{-29} cm^2 keV.

The possibility that these unexpectedly large channels for the photoexcitation of isomers were the results of poor calibrations of fluxes was minimized by the use of four different accelerators in diverse environments and by the fact that the yields of the reaction $^{87}\mathrm{Sr}(\gamma,\gamma')^{87}\mathrm{Sr}^m$ up to 4 MeV were completely explained by the accepted values of integrated cross sections. Contamination of the products by activations from photoneutrons was shown to be generally less than 1%. It would seem that these enhanced channels for (γ,γ') reactions are the results of surprisingly favorable transitions to intermediate states that can be excited at energies less than 4 MeV. Earlier works reported in the literature were generally limited to 3 MeV and did not find activations of this magnitude, so it would be reasonable to speculate that these highly favored channels might lie between 3 and 4 MeV above the ground state.

While the ratios of activations found with 4 MeV bremsstrahlung to that produced around 1 MeV were of the order of thousands, the further increases from 4 to 6 MeV were much smaller. In Table II, the quantity κ_1 summarizes the increases in activation produced by raising the end point from 4 to 6 MeV and the quantity κ_2 records the further change resulting from an increase from 6 to 10 MeV. With a few obvious exceptions, the general trend supports the hypothesis that the principal nuclear structure responsible for the order-of-magnitude enhancement of (γ,γ') reactions lies below 4 MeV. Much smaller increases occur between 4 and 6 MeV and perhaps none between 6 and 10 MeV. Despite the care taken in reconciling the different environments, values of $0.7 \leq \kappa_2 \leq 1.5$ are probably not significantly different from unity. There is no persuasive evidence that additional channels opened between 6 and 10 MeV. In turn, this seems to imply that the giant dipole resonances have nothing to do with the enhancement of these (γ,γ') reactions.

The difficulties in explaining the sizes of the integrated cross sections reported in this work accrue from the large changes in angular momentum, J separating ground states from isomers. Most of the larger values belong to nuclei which are spheroidal and the projections of angular momentum, K, upon the axes of elongation differ greatly in ground and isomeric states. With an absorption transition of reasonable probability, changes in J and K are limited to $\Delta J \leq 2$ and $\Delta K \leq 2$. While the first might be satisfied by making a transition from the ground state to a high member of a rotational band built upon the final state, the second would be violated because K is conserved within a rotational band. What is needed is a mechanism to mix K values of nuclear levels belonging to rotational bands built upon initial and final states of the (γ,γ') reaction.

It is interesting to speculate that this might occur as a result of couplings to states built upon cores of nonfissioning shape isomers.[23] Such states show double minima in energy as functions of elongation, even at low values of spin. At some values of excitation energy the shape of such a nucleus would be unstable and projections upon its principal axes would no longer be conserved. In this way the transition from a K value characteristic of the ground state to one consistent with the isomer might occur by mixing with such a state. In any case the frequency with which giant values of integrated cross sections for photoexcitation were found in this work argues for some type of core property varying slowly with increasing nuclear size. Further work is needed to resolve the precise cause of this phenomenon.

This work was supported by the Strategic Defense Initiative Organization/Innovative Science and Technology Directorate and directed by the Naval Research Laboratory.

*Present address: High Energy Laser Associates, Oakland, CA 94611.
†Present address: Plasma Physics Department, Soreq Nuclear Research Center, Israel.
‡Present address: The University of Texas Southwestern Medical Center, Dallas, TX 75235.

[1]See, for example, the review, S. S. Dietrich and B. L. Berman, At. Data Nucl. Data Tables **38**, 199 (1988).
[2]B. Pontecorvo and A. Lazard, C. R. Acad. Sci. **208**, 99 (1939).
[3]G. B. Collins, B. Waldman, E. M. Stubblefield, and M. Goldhaber, Phys. Rev. **55**, 507 (1939).
[4]Y. Watanabe and T. Mukoyama, Bull. Inst. Chem. Res., Kyoto Univ. **57**, 72 (1979).
[5]M. Krcmar, A. Ljubicic, K. Pisk, B. Logan, and M. Vrtar, Phys. Rev. C **25**, 2097 (1982).
[6]I. Bikit, J. Slivka, I. V. Anicin, L. Marinkov, A. Ruydic, and W. D. Hamilton, Phys. Rev. C **35**, 1943 (1987).
[7]M. Krcmar, A. Ljubicic, B. A. Logan, and M. Bistrovic, Phys. Rev. C **33**, 293 (1986).
[8]E. B. Norman, S. E. Kellogg, T. Bertram, S. Gil, and P. Wong, Astrophys. J. **281**, 360 (1984).
[9]J. A. Anderson and C. B. Collins, Rev. Sci. Instrum. **58**, 2157 (1987).
[10]J. A. Anderson and C. B. Collins, Rev. Sci. Instrum. **59**, 414 (1988).
[11]Walter R. Nelson, Hideo Hirayama, and David W. O. Roger, SLAC Report 265, 1985.
[12]J. A. Halbleib and T. A. Mehlhorn, Sandia National Laboratories Report SAND84-0573, 1984.
[13]J. A. Anderson, M. J. Byrd, and C. B. Collins, Phys. Rev. C **38**, 2833 (1988).
[14]C. B. Collins, J. A. Anderson, Y. Paiss, C. D. Eberhard, R. J. Peterson, and W. L. Hodge, Phys. Rev. C **38**, 1852 (1988).
[15]*Evaluated Nuclear Structure Data File,* Information Analysis Center Report BNL-NC5-51655 (Brookhaven National Laboratory, Upton, New York, 1983).
[16]C. B. Collins, C. D. Eberhard, J. W. Glesener, and J. A. Anderson, Phys. Rev. C **37**, 2267 (1988).
[17]J. J. Carroll, J. A. Anderson, J. W. Glesener, C. D. Eberhard, and C. B. Collins, Astrophys. J. **344**, 454 (1989).
[18]C. B. Collins, J. J. Carroll, T. W. Sinor, M. J. Byrd, D. G. Richmond, K. N. Taylor, M. Huber, N. Huxel, P. v. Neumann-Cosel, A. Richter, C. Spieler, and W. Ziegler, Phys. Rev. C **42**, 1813 (1990).
[19]E. C. Booth and J. Brownson, Nucl. Phys. **A98**, 529 (1967).
[20]B. Bernstein and I. B. Smith, IEEE Trans. Nucl. Sci. **NS-20**, 294 (1973).
[21]R. Mohan, C. Chui, and L. Lidofsky, Med. Phys. **12**, 595 (1985).
[22]*ASTM Standard Method for Determining Thermal Neutron Reaction and Fluence Rates by Radioactivation Techniques,* Publication E 262-86 (American Society for Testing and Materials, Philadelphia, 1987), and references cited there.
[23]M. Girod, J. P. Delaroche, D. Gogny, and J. F. Berger, Phys. Rev. **62**, 2452 (1989).